Chinese Chemical Letters 34 (2023) 107983

Contents lists available at ScienceDirect

Chinese Chemical Letters

journal homepage: www.elsevier.com/locate/cclet

Exploring the influence of crystal packing on the optical-physical property of quercetin-based binary and ternary solid forms

Zhonghua Li[a,1], Jianmin Zhou[a,1], Xin Zhang[a], Songgu Wu[a,*], Junbo Gong[a,b,c,*]

[a] State Key Laboratory of Chemical Engineering, School of Chemical Engineering and Technology, Tianjin University, Tianjin 300072, China
[b] Chemistry and Chemical Engineering Guangdong Laboratory, Shantou 515031, China
[c] Haihe Laboratory of Sustainable Chemical Transformations, Tianjin 300192, China

ARTICLE INFO

Article history:
Received 8 September 2022
Revised 28 October 2022
Accepted 3 November 2022
Available online 5 November 2022

Keywords:
Natural plant pigment
Cocrystal
Solvate
Crystal structure
Molecular conformation
Intermolecular interaction

ABSTRACT

The co-crystallization of quercetin (Qur) with a flexible molecule 4-(4-pyridinyldisulfanyl) pyridine (DPDS) in different solvents and conditions was investigated, yielded five multi-component crystalline phases and characterized with X-ray diffractions and thermal analysis. Although the crystal system of Qur-DPDS-MeOH and Qur-DPDS-Dioxane is the same, the desolvation results revealed that Qur-DPDS-MeOH transformed to Qur-DPDS when MeOH solvent molecules escape from the lattice, while Qur-DPDS-Dioxane transformed to Qur-DPDS-II through a similar process, which is same with Qur-DPDS-THF. These two cocrystal polymorphs Qur-DPDS and Qur-DPDS-II obey an enantiotropic relationship. Moreover, the formation of cocrystal solvates improves the packing efficiency of crystals. Crystal structure analysis showed that hydrogen bonds and conformations of the corresponding parent molecules play a major role in molecular assembly and crystal packing patterns, thus bring different physicochemical properties. Finally, the fluorescence spectra and quantum-chemical calculations were carried out to explore the difference in the optical-physical properties.

Quercetin (Fig. 1, Qur) belongs to an important biological flavonoid, widely used in the nutraceutical industry and as a food supplement [1]. Qur primarily possesses anti-inflammatory, antioxidative, and antibacterial properties, which can be extracted from natural plants [2,3]. It has also been demonstrated that Qur shows outstanding potential to inhibit tumor growth [4]. In addition, what is often overlooked is that Qur itself is also a natural plant pigment, its powder having bright yellow color and fluorescing when exposed to ultraviolet light [5]. Because of its wide range of biological effects and good optical properties, Qur has attracted continuous attention from researchers [6–8]. Many luminescent crystal materials with excellent properties have been reported to promote the practical application [9–11]. However, it is still challenging to select suitable molecules to prepare cocrystal to meet specific requirements [12–14].

Previous works [15–18] described a range of polymorphs, hydrates, solvates and cocrystals of Qur, and focused on improving its biologically relevant properties, such as dissolution rate, bioavailability, and biological activity. Surprisingly, there has been relatively little study to explore other possible solid forms of Qur to modulate the optical-physical properties up to now. More than 40 Qur-related crystal structures have been collected in the CCDC database, and it is not difficult to find that the existence of multiple hydrogen bond donor and acceptor sites in the structure of Qur as well as flexible molecular conformation create convenient conditions for the supramolecular assembly and crystal packing. Desiraju and co-workers [19] obtained 28 cocrystals of Qur with six dibasic coformers based on crystal engineering strategy. To further investigate the effect of molecular conformations on crystal structures and properties, we had the idea of introducing a flexible molecule DPDS (Fig. 1) as a coformer to participate in the co-crystallization of Qur based on the robust O-H···N synthon. Our objective was to identify new multi-component crystals of Qur with adjustable optical properties. DPDS is one of the coformers most frequently selected for co-crystallization trials, and some cocrystals with DPDS have been reported [20–22].

Here, two cocrystal polymorphs comprising Qur and DPDS and three cocrystal solvates involving solvents were obtained and characterized by powder X-ray diffraction (PXRD), thermogravimetric analysis (TGA), and differential scanning calorimetry (DSC). The process of solvent escape from the lattice of ternary cocrystal

---

[*] Corresponding authors at: State Key Laboratory of Chemical Engineering, School of Chemical Engineering and Technology, Tianjin University, Tianjin 300072, China.

E-mail addresses: wusonggu@tju.edu.cn (S. Wu), junbo_gong@tju.edu.cn (J. Gong).

[1] These authors contributed equally to this work.

https://doi.org/10.1016/j.cclet.2022.107983

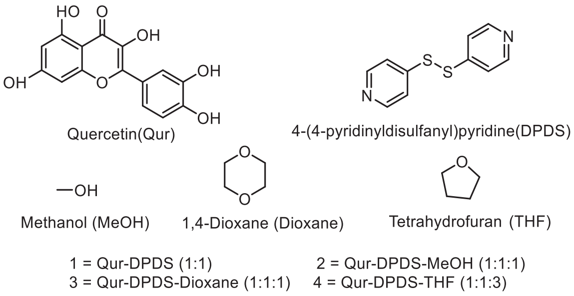

Fig. 1. Molecular structures of Qur, DPDS and the related solvents.

was monitored *via* hot-stage microscopy (HSM). The crystal structures of four multi-component crystals were determined by single-crystal X-ray diffraction (SCXRD). Moreover, molecular conformation and crystal stacking modes, intermolecular interactions and energy were conducted for detailed comparisons. For a given organic luminescent component, the strategy based on the cocrystal solvates can not only modify the optical properties by regulating fluorophores stacking arrangements but also help to find more cocrystal polymorphic phases. Finally, the difference in luminescent properties was rationalized with the calculation of the HOMO-LUMO gaps. The raw materials, specific experimental procedures, solid-state characterization methods, and computational details were shown in the Supporting information.

The corresponding crystallographic data and hydrogen bond parameters of the obtained cocrystal and cocrystal solvates of Qur with DPDS are presented in Tables S1 and S2 (Supporting information), respectively. Qur-DPDS (Fig. 2a) cocrystal crystallized in the orthorhombic crystal system with the space group of *P*bcn, the asymmetry unit includes one Qur molecule and one DPDS molecule. A series of intramolecular hydrogen bonds $O_2\text{-}H_2{\cdots}O_3$, $O_4\text{-}H_4{\cdots}O_3$, and $O_6\text{-}H_6{\cdots}O_7$ existed in Qur molecules. Typical dimers were formed between Qur molecules *via* a $R_2^2(4)$ supramolecular synthon through $O_4\text{-}H_4{\cdots}O_7$ and $O_6\text{-}H_6{\cdots}O_3$ interactions, then Qur dimers formed a wavy 1D structure along *a*-axis. DPDS molecules help different 1D chains to construct the 2D structure in the *ac* plane *via* $O_1\text{-}H_1{\cdots}N_1$ and $O_7\text{-}H_7{\cdots}N_2$ hydrogen bonds.

Qur-DPDS-MeOH (Fig. 2b) solvate has a monoclinic crystal system and space group $P2_1/c$. The asymmetry unit contains one molecule each of Qur, DPDS and MeOH molecules. Qur molecule connected to three DPDS molecules by the $O_1\text{-}H_1{\cdots}N_2$ and $O_7\text{-}H_7{\cdots}N_1$ strong hydrogen bonds and $O_6\text{-}H_6{\cdots}S_2$ weak hydrogen bonds, meanwhile, O-H···O hydrogen bonds link Qur molecule and MeOH molecules. Qur molecules are linked by the $O_6\text{-}H_6{\cdots}O_1$ hydrogen bond, forming a 1D structure along the *b*-axis. Both DPDS molecules and MeOH molecules connect Qur molecules to each other along the *a*-axis, promoting the formation of a 2D structure.

Qur-DPDS-Dioxane (Fig. 2c) solvate crystallized in the monoclinic crystal system with the space group of $P2_1/c$. Two Qur molecules are anchored between DPDS molecules through $O_6\text{-}H_6{\cdots}N_1$ and $O_7\text{-}H_7{\cdots}N_2$ interactions, which help the formation of the tetramer. Besides, it can be obviously observed that 1,4-dioxane molecules are wrapped in the cavity formed by the tetramer, in which there are only weak C-H···O hydrogen bonds between solvent molecules and Qur molecules. Qur molecules are connected to each other through $O_1\text{-}H_1{\cdots}O_7$ hydrogen bonds to form an infinite 1D chain along the *b*-axis. A sandwich structure is observed in the *bc* plane, which is composed of two antiparallel Qur chains, face-to-face DPDS molecule pairs and 1,4-dioxane molecules in the cavity. The sandwich structure is further connected through $O_4\text{-}H_4{\cdots}O_2$ hydrogen bonds and expanded into a 2D planar structure.

Qur-DPDS-THF (Fig. 2d) solvate forms in the orthorhombic crystal system with the space group of *P*bca, including one Qur molecule, one DPDS molecule, and three THF molecules in the asymmetry unit, different from two previous solvates. Qur molecule is linked with three THF molecules through the $O_6\text{-}H_6{\cdots}O_8$, $O_7\text{-}H_7{\cdots}O_{10}$, and $C_9\text{-}H_9{\cdots}O_9$ hydrogen bonds. Different from the other crystal structures, there are no typical O-H···O interactions between Qur molecules in Qur-DPDS-THF solvate. Instead, $O_1\text{-}H_1{\cdots}N_1$ and $O_4\text{-}H_4{\cdots}N_2$ interactions along the *c*-axis assisted by DPDS molecules play an important role to link the Qur molecules together.

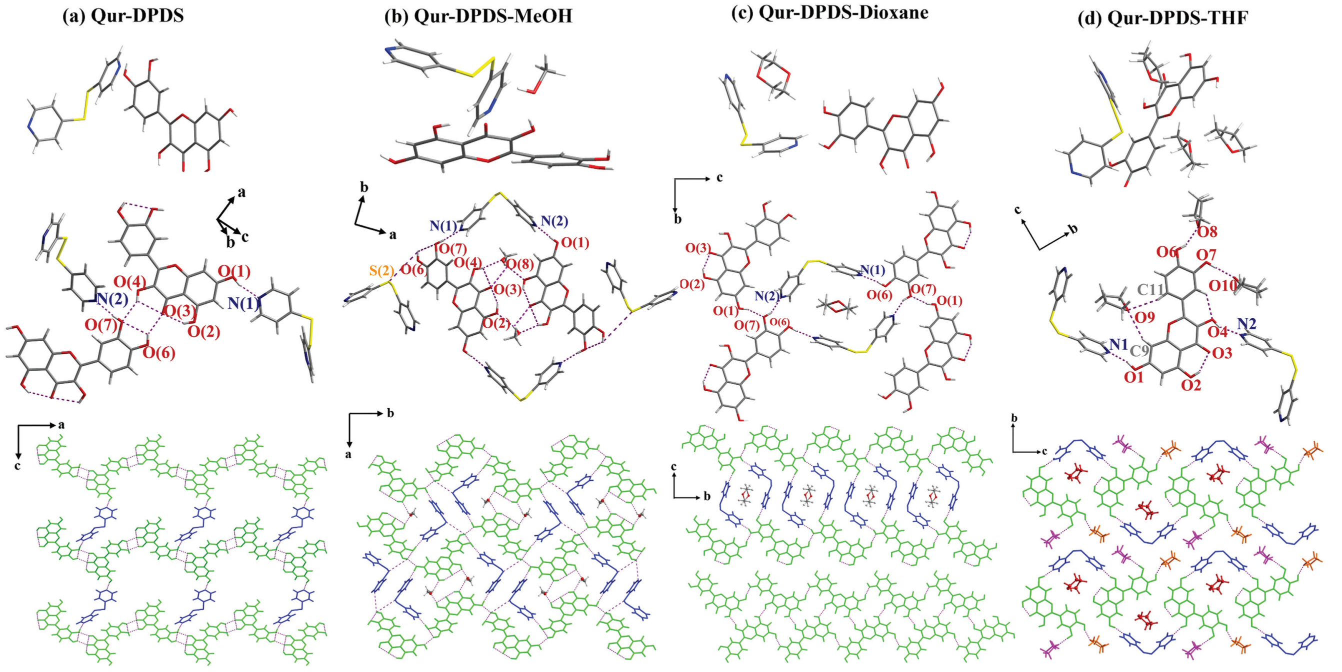

Fig. 2. The asymmetric units, hydrogen bond motifs, and packing modes of the crystal structures in (a) Qur-DPDS, (b) Qur-DPDS-MeOH, (c) Qur-DPDS-Dioxane and (d) Qur-DPDS-THF.

The main difference between these three cocrystal solvates and the cocrystal lies in the conformation of the Qur molecule and the DPDS molecule. Figs. S1a and b (Supporting information) show the overlay of the Qur conformations and DPDS conformations in different Qur-related multi-component crystals, respectively. Table S3 (Supporting information) lists the main torsion angles τ_1 and τ_2. It is obvious that the conformations of Qur molecules in different solid forms are completely different, reflected in the orientation of the hydroxyl groups at multiple sites on the one hand, and in the torsion angle of the phenyl to the pyrone ring on the other. Desiraju *et al.* [19] described 12 possible conformations by calculations, and five of these conformations were observed containing Conf 1B, 2A, 5B, 6B and 7B, surprisingly, the relatively stable conformation (Conf 2B) did not appear. Moreover, the emergence of Conf 2B is also a low probability event among over 40 Qur-related crystal structures in CCDC. Referring to the naming of conformations for Qur by Desiraju and coworkers, we found that four conformations were obtained in our study, including two common conformations (Conf 5B and 6B) and two rarely found conformations (Conf 2A and 2B). Furthermore, the conformation of DPDS in Qur-DPDS cocrystal is different from those in Qur-DPDS cocrystal solvates, and the conformations of DPDS in Qur-DPDS-Dioxane and Qur-DPDS-THF are particularly similar. DFT calculation for conformations was conducted by Gaussian with two different basis sets, the results of conformation energy in multi-component crystals suggested the conformation of Qur in Qur-DPDS-THF and the conformation of DPDS in Qur-DPDS-MeOH are more stable, while the conformations of Qur and DPDS in Qur-DPDS have high energy. This may provide an explanation for the difficulty in obtaining Qur-DPDS cocrystal with solution crystallization. In our experiments, Qur-DPDS powder samples were obtained by the desolvation of Qur-DPDS-MeOH, while its single crystal was successfully cultured only once among several attempts with slow evaporation. In addition, another reason is due to that the crystal packing efficiency [23] is improved through the formation of cocrystal solvates, in detail, Qur-DPDS 59.8%, Qur-DPDS-MeOH 69.2%, Qur-DPDS-Dioxane 72.7%, and Qur-DPDS-THF 69.4%. It can be revealed that in this system, the generation of multi-component crystals has an obvious influence on the conformation of the host molecule and coformer molecule, which further affects the crystal assembly.

To characterize and discuss the intermolecular interactions, Hirshfeld surfaces [24] calculation mapped over d_{norm} (Fig. S2a in Supporting information) was carried out. The bright red spots (negative electrostatic potential) indicated the presence of O-H···O close contact interaction, and the blue regions (positive electrostatic potential) over the Hirshfeld surfaces act as hydrogen donors. Meanwhile, the red regions of shape index surface plots (Fig. S2b in Supporting information) [25] represents the C-H···π and π···π interactions. The relative contribution of the intermolecular contacts *via* 2D fingerprint plots were also summarized in Fig. S2c (Supporting information). Three dominant atom interactions are the H-H and O-H interaction types in all the four crystals of Qur. Meanwhile, the O-H interaction is related to O-H···O and O-H···N hydrogen bonds. It is worth notable that some weak interactions also have a considerable proportion and play an important role in the stacking of crystal structures, such as C-H, S-H, C-C interaction types. The π-stacking dimers in crystal packing patterns were extracted from the related crystal structures, and the π-π interactions were evaluated accurately by interaction energy calculations. As shown in Figs. S2d-f (Supporting information), the interaction energy of Qur-Qur pairs from Qur-DPDS-Dioxane is larger than that from Qur-DPDS and Qur-DPDS-MeOH.

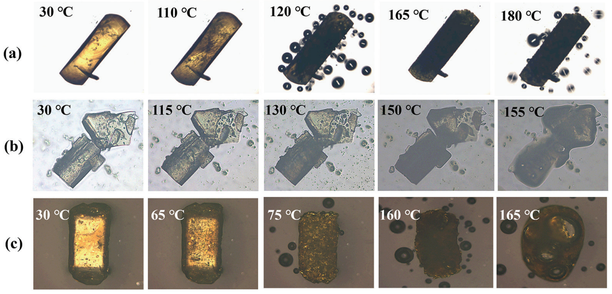

Fig. 3. HSM images for (a) Qur-DPDS-MeOH, (b) Qur-DPDS-Dioxane, (c) Qur-DPDS-THF.

PXRD is an effective means to identify new solid-state forms, as shown in Fig. S3 (Supporting information), each measured PXRD pattern of the obtained Qur cocrystal and cocrystal solvates bulk powder is distinct from those of their starting materials. Meanwhile, these experimental PXRD patterns are closely match with those corresponding simulated patterns from single crystal data, indicating the formation of highly pure phases. The thermal stability of the obtained Qur-related multi-component crystals was evaluated by TGA and DSC, and the results are shown in Fig. S4 (Supporting information). The TGA plot of Qur-DPDS shows no weight loss before the decomposition, indicating no solvents are involved in its crystal structure. It is in accordance with the DSC curve exhibiting only one endotherm peak, which corresponds to the melting point of Qur-DPDS. However, the remaining three multi-component crystals are found to have different thermal behaviors from Qur-DPDS, at least one thermic peak representing the release of the corresponding solvent appears before they melt. As summarized in Table S4 (Supporting information), the starting temperature of desolvation for Qur-DPDS-THF is lower than Qur-DPDS-MeOH and Qur-DPDS-Dioxane, probably influenced by two factors including solvent boiling point and intermolecular interactions. The more detailed thermal behavior of Qur-related cocrystal solvates was recorded *via* HSM, containing desolvation, melting and decomposition (Figs. 3a-c). The desolvation temperature shown in HSM is consistent with that presented in DSC plots. Furthermore, TGA reveals the consistency of solvent stoichiometry calculated from the curves and the results determined by SCXRD for these three Qur cocrystal solvates. The PXRD patterns of different desolvated samples were also be characterized (Fig. 4a). The results show that Qur-DPDS-MeOH transform to Qur-DPDS after desolvation, and the PXRD patterns of the desolvated products for Qur-DPDS-Dioxane and Qur-DPDS-THF are same but different from the obtained Qur-DPDS. In other words, a new cocrystal polymorph Qur-DPDS-II was discovered with the help of the desolvation of the specific solvate. Meanwhile, the T_{onset} for Qur-DPDS is 166.10 °C, and the corresponding fusion heat is 93.08 J/g. As shown in Fig. S5 (Supporting information), DSC curve of Qur-DPDS-II indicates melting at T_{onset} of 152.63 °C, and the heat of fusion is 127.26 J/g. Qur-DPDS and Qur-DPDS-II obey an enantiotropic relationship according to Burger and Ramberger's heat of fusion rule [26]. FT-IR spectroscopy and EA were also used to demonstrate the characteristics of various crystalline forms (Fig. S6 and Table S5 in Supporting information).

Subsequently, the corresponding fluorescence spectra were recorded to explore the luminescent properties, and the results (Figs. 4b-d) show that the emission wavelength of Qur-DPDS-II (600nm) is red-shifted compared with Qur-DPDS (586 nm). Moreover, it can be observed that the emission wavelength of Qur-DPDS-MeOH is blue-shifted after the desolvation (Qur-DPDS-MeOH, 597 nm; Qur-DPDS, 586 nm). However, as a comparison, the emission wavelength of Qur-DPDS-Dioxane is almost unchanged when 1,4-dioxane solvent molecules escape from the original crystals (Qur-DPDS-Dioxane, 601 nm; Qur-DPDS-II, 600 nm). The variation in emission wavelength is mainly attributed to the packing patterns of molecules and intermolecular interactions in crystals. Combining the fluorescence emission spectra (Fig. 4d) and

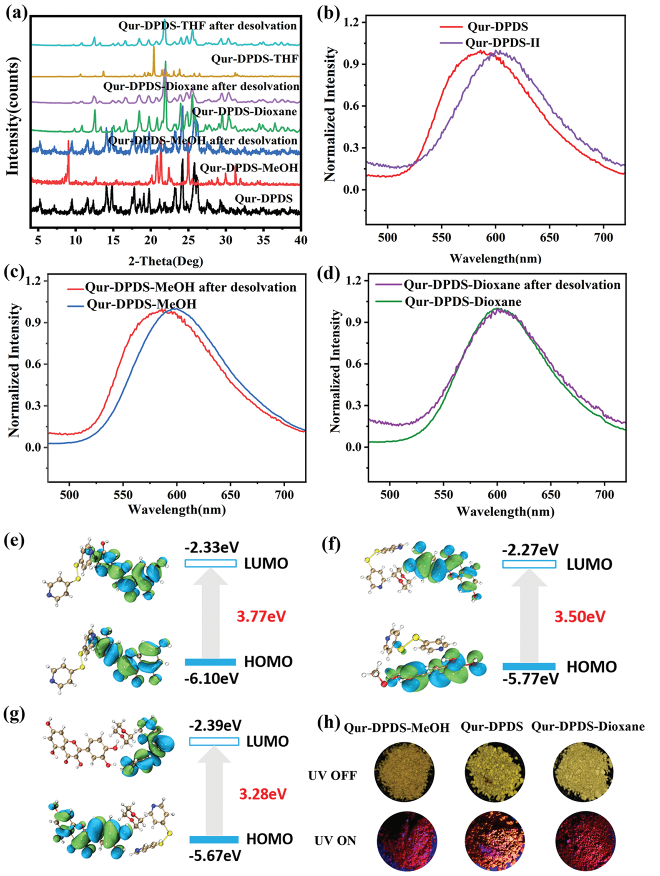

Fig. 4. (a) PXRD patterns of the desolvation process of three Qur-DPDS cocrystal solvates, and normalized fluorescence spectra of (b) Qur-DPDS, Qur-DPDS-II (c) Qur-DPDS-MeOH, Qur-DPDS and (d) Qur-DPDS-Dioxane, Qur-DPDS-II, and molecular orbital diagrams and isodensity surface plots of the HOMOs and LUMOs of (e) Qur-DPDS, (f) Qur-DPDS-MeOH, (g) Qur-DPDS-Dioxane in their ground states, (h) photos of Qur-DPDS, Qur-DPDS-MeOH, and Qur-DPDS-Dioxane under visible light and 365 UV.

the PXRD patterns (Fig. 4a) before and after desolvation of the cocrystal solvate, we can preliminarily infer that the crystal structures of Qur-DPDS-Dioxane and Qur-DPDS-II may be similar, and they are likely to belong to isostructural crystals. Furthermore, to better understand the change of the optical-physical properties, DFT calculations were performed, for Qur-DPDS and Qur-DPDS-MeOH, the distribution of the electron cloud is only located in Qur molecules (Figs. 4e and f). Moreover, it can be seen that for Qur-DPDS-Dioxane, the highest occupied molecular orbital (HOMO) is located on Qur moiety, while the lowest unoccupied molecular orbital (LUMO) is distributed on DPDS moiety (Fig. 4g). The calculated HOMO-LUMO energy gaps can be turned from 3.77 eV to 3.28 eV, attributed to the changes in electron donor and acceptor energy levels. The color of the corresponding powder samples of Qur-DPDS, Qur-DPDS-MeOH, and Qur-DPDS-Dioxane is a little different, reflected in the photos under visible light (Fig. 4h). When the samples are irradiated with UV light, Qur-DPDS show a significantly different fluorescence color from Qur-DPDS-MeOH and Qur-DPDS-Dioxane.

In summary, the co-crystallization of Qur with DPDS affords three cocrystal solvates and two cocrystals. The detailed comparisons of the crystal structures, intermolecular hydrogen bonding interactions, and emission properties of the corresponding solid forms were discussed. The analysis of molecular conformation reveals that Qur molecule in the multi-component crystals exhibited significant differences, and the conformation energy of Qur and DPDS in Qur-DPDS cocrystal are relatively high compared to the other crystals. In addition, the desolvation process of three cocrystal solvates was analyzed in detail *via* various characterization tools, and the cocrystal polymorphic phase Qur-DPDS-II was accidentally isolated after the desolvation of Qur-DPDS-Dioxane and Qur-DPDS-THF. Finally, the solid-state emission properties of Qur-DPDS-related crystals were compared and rationalized with theoretical calculations. The results show that the molecular packing structures of the crystals will have a dramatic effect on the optical-physical properties. Discovering novel and suitable phases based on crystal engineering strategy will be helpful to obtain desired properties and expand the potential applications.

Declaration of competing interest

The authors declare no competing financial interest.

Acknowledgment

This work was financially supported by the National Natural Science Foundation of China (Nos. 22178254 and 21621004).

Supplementary materials

Supplementary material associated with this article can be found, in the online version, at doi:10.1016/j.cclet.2022.107983.

References

[1] A.J. Smith, P. Kavuru, L. Wojtas, M.J. Zaworotko, R.D. Shytle, Mol. Pharm. 8 (2011) 1867–1876.
[2] G.S. Kelly, Altern. Med. Rev. 16 (2011) 172–195.
[3] P. Lakhanpal, D.K. Rai, Int. J. Med. 2 (2007) 22–37.
[4] S.M. Tang, X.T. Deng, J. Zhou, et al., Biomed. Pharmacother. 121 (2020) 109604.
[5] P.M. Shah, V.V. Priya, R. Gayathri, J. Pharm. Sci. Res. 8 (2016) 878.
[6] T. Hatahet, M. Morille, A. Hommoss, et al., Eur. J. Pharm. Biopharm. 102 (2016) 51–63.
[7] A. Masek, M. Latos, M. Piotrowska, M. Zaborski, Food Packag. Shelf Life 16 (2018) 51–58.
[8] I. García-Casas, A. Montes, C. Pereyra, E.J. Martínez de la Ossa, Eur. J. Pharm. Sci. 100 (2017) 79–86.
[9] B. Lu, S. Liu, D. Yan, Chin. Chem. Lett. 30 (2019) 1908–1922.
[10] Y. Lu, Y. Tang, H. Lin, et al., Chin. Chem. Lett. 29 (2018) 1541–1543.
[11] S. Li, B. Lu, X. Fang, D. Yan, Angew. Chem. Int. Ed. 59 (2020) 22623–22630.
[12] D. Yan, D.G. Evans, Mater. Horiz. 1 (2014) 46–57.
[13] G. Xiao, X. Fang, Y. Ma, D. Yan, Adv. Sci. 9 (2022) 2200992.
[14] F. Nie, B. Zhou, K. Wang, D. Yan, Chem. Eng. J. 430 (2022) 133084.
[15] X. Filip, I.G. Grosu, M. Miclăuş, C. Filip, CrystEngComm 15 (2013) 4131–4142.
[16] K. Srinivas, J.W. King, L.R. Howard, J.K. Monrad, J. Food Eng. 100 (2010) 208–218.
[17] P. Klitou, C.M. Pask, L. Onoufriadi, I. Rosbottom, E. Simone, Cryst. Growth Des. 20 (2020) 6573–6584.
[18] F. Liu, L.Y. Wang, M.C. Yu, et al., Eur. J. Pharm. Sci. 144 (2020) 105216.
[19] R. Dubey, G.R. Desiraju, IUCrJ 2 (2015) 402–408.
[20] Q. Zeng, D. Wu, H. Ma, C. Shu, Y. Li, C. Wang, CrystEngComm 8 (2006) 189–201.
[21] D.J. Wang, J.M. Zhao, J. Zhang, J.L. Lin, Acta Crystallogr. Sect. E 65 (2009) o1055-o1055.
[22] L. Fang, Y. Ma, Y. Xiao, et al., Cryst. Growth Des. 22 (2022) 1707–1719.
[23] A. Berzins, E. Skarbulis, T. Rekis, A. Actins, Cryst. Growth Des. 14 (2014) 2654–2664.
[24] M.A. Spackman, D. Jayatilaka, CrystEngComm 11 (2009) 19–32.
[25] P.R. Spackman, M.J. Turner, J.J. McKinnon, et al., J. Appl. Crystallogr. 54 (2021) 1006–1011.
[26] A. Burger, R. Ramberger, Microchim. Acta 72 (1979) 259–271.